Rare Metal Materials and Engineering
Volume 51, Issue 3, March 2022
Available online at www.rmme.ac.cn

Science Press

Cite this article as: Gao Shan, Zou Jianpeng. Oxidation Resistance Behavior of NiAl Coating on NiCrW-based Superalloy by Pack Cementation[J]. Rare Metal Materials and Engineering, 2022, 51(03): 814-820.

ARTICLE

Oxidation Resistance Behavior of NiAl Coating on NiCrW-based Superalloy by Pack Cementation

Gao Shan[1], Zou Jianpeng[1,2]

[1] State Key Laboratory of Powder Metallurgy, Central South University, Changsha 410083, China; [2] State Key Laboratory for System Integration of High Power AC Drive Electric Locomotive, Zhuzhou 412001, China

Abstract: The NiAl coating was prepared on the surface of NiCrW-based superalloy by pack cementation method with $CaCl_2$ as an activator. The surface and cross-section of the coated specimens were analyzed via X-ray diffraction and scanning electron microscopy coupled with energy dispersive spectroscopy. Results show that $CaCl_2$ can replace NH_4Cl as an effective activator. The NiAl coating with an almost single phase structure and a thickness of 30 μm can be obtained after pack cementation at 950 °C for 4 h. A chromium-rich interlayer can be observed between the NiAl coating and the substrate. When the filling ratio of the pack powder is less than 100%, the needle-like θ-Al_2O_3 phase is formed on the NiAl layer surface. During the constant temperature air oxidation test at 1000 °C, the NiAl coating suffers from high speed oxidation to slow speed oxidation, which is in agreement with the phase transformation from needle-like metastable θ-Al_2O_3 to irregular granular stable α-Al_2O_3. The final stable α-Al_2O_3 provides a good oxidation resistance for the substrate.

Key words: NiCrW-based superalloy; NiAl coating; pack cementation; oxidation resistance

Nickel-based superalloys play a key role in the manufacturing of combustion chambers, rocket tail nozzles, and heat exchange tubes for high-temperature gas-cooled reactors[1]. However, in recent years, the difficulty of increasing the melting point of metal materials has restricted the maximum operating temperature of the engine turbine inlet[2]. Therefore, the development of high-temperature protection technique for nickel-based superalloys is essential.

Typically, the high temperature coatings, including the normal coating and the diffusion coating, can protect the Ni-based superalloys[3] no matter it reacts with the substrate or not[4]. At present, the main coating preparation methods on the alloy substrate include the pack cementation, hot-dipping, chemical vapor deposition, and molten salt techniques[5,6]. The pack cementation method has been widely used due to its low production cost, simple operation, simple equipment, good effect of infiltration layer, and strong binding force between the coating and the substrate[7]. Both the NiAl coatings and modified γ-Ni+γ'-Ni_3Al coatings with excellent properties can be prepared by pack cementation[8]. Several studies studied the preparation of aluminized coatings via pack cementation[9,10]. However, the phase formation and microstructure evolution of the coating on the superalloy substrate during the pack cementation are still unclear. The evolution behavior and formation mechanism should be further investigated because they are essential for the practical application of coatings.

The structure and properties of the coating prepared by pack cementation are related to the chemical composition of the substrate[11] and the composition and filling ratio of the pack powder. Zielinska et al[12] found that the superalloys with high total contents of Ni and Co and low contents of Cr, Mo, W, and Ti have thick aluminide layers. It is also found that the aluminide layer can be prepared in $AlCl_3$ vapor with hydrogen as the carrier gas, and the corrosion resistance of the substrate can be further improved in the mixture of $AlCl_3$+$ZrCl_3$ vapor[13,14]. In addition, the partial pressure of AlCl, $AlCl_2$, and $AlCl_3$ can be controlled by the HCl/H_2 ratio in the initial gas stream, thereby controlling the growth of the aluminide layer[15]. However, the research on aluminizing in closed environment is still not comprehensive.

Received date: March 07, 2021
Foundation item: Natural Science Foundation of Hunan Province (2018JJ2524)
Corresponding author: Zou Jianpeng, Ph. D., Professor, State Key Laboratory of Powder Metallurgy, Central South University, Changsha 410083, P. R. China, Tel: 0086-731-88876630, E-mail: zoujp@csu.edu.cn

Copyright © 2022, Northwest Institute for Nonferrous Metal Research. Published by Science Press. All rights reserved.

Lu et al[16] investigated the low-temperature formation of aluminide coatings on a Ni-based superalloy through pack cementation with NH_4Cl as an activator, and found that the NH_4Cl content affects neither the coating thickness nor the structure or component distribution. However, the heating and decomposition of NH_4Cl will generate toxic ammonia gas and HCl gas, which may corrode the production equipment.

Therefore, the NiAl coating with a controllable structure was prepared under different filling ratios of pack powder with an environmental-friendly activator $CaCl_2$ in this research. The air constant temperature oxidation experiment was performed at 1000 °C and the oxidation resistance behavior of the NiCrW-based superalloy with NiAl coating was investigated.

1 Experiment

The as-cast NiCrW-based superalloy was used as the substrate, and its main chemical composition is shown in Table 1. The NiCrW-based superalloys were cut into specimens of 10 mm×10 mm×5 mm. The specimens were polished by 320#, 800#, 1200#, and 2000# sandpapers, cleaned by acetone, and then dried. The pack powders were composed of 20wt% Al (reactor, 38~75 μm), 2wt% $CaCl_2$ (activator), 77wt% Al_2O_3 (inert filler, 150~250 μm), and 1wt% CeO_2 (<5 μm). Moreover, the Al_2O_3 powder was calcined at 1200 °C for 2 h to remove the substances of low melting point. These powders were mixed in proportion thoroughly in a grinding machine, and then placed in the corundum crucible with the specimens. The pack powder with the filling ratio of 100%, 90%, 70%, and 50% was used and then sealed with fire-resistant mud. The sealed crucible was placed in a drying oven at 120 °C for 4 h. Furthermore, the muffle furnace was heated to 950 °C at a heating rate of 10 °C/min. The specimens were heated at 950 °C for 4 h in the furnace and then cooled naturally. The coating phase was determined via X-ray diffraction (XRD, D/max2550). In addition, the cross-section morphology and the element content of the coating were evaluated via scanning electron microscopy (SEM, FEI Quanta250FEG) coupled with energy dispersive spectroscopy (EDS).

Discontinuous weighing method was used in the constant temperature oxidation test, and the oxidation medium was air. Before the test, the initial mass of the specimen was weighed by an electronic analytical balance. Then the specimen was placed in an alumina crucible and put into a muffle furnace for heat preservation at 1000 °C for 2, 5, 10, 20, 50, 100, 150, and 200 h. The crucible was taken out at 2, 5, 10, 20, 50, 100, 150, and 200 h, separately, and the specimen was weighed after natural cooling. The mass gain curve per unit surface area of the specimen was used to evaluate the high temperature oxidation resistance of the coating. The related formula is as follows:

$$\Delta W = \frac{M - m}{S} \quad (1)$$

where ΔW is the oxidation mass gain per unit area ($mg \cdot cm^{-2}$); M is the specimen mass at different time (mg); m is the initial specimen mass (mg); S is the surface area of the specimen (cm^2).

Table 1 Main composition of as-cast NiCrW-based superalloys (wt%)

Cr	W	Co	Mo	Al	C	Ni
18.860	16.130	11.850	1.280	0.820	0.084	50.410

2 Results and Discussion

2.1 Morphology and phase component of NiAl coatings

Fig. 1 shows XRD pattern of NiAl coating with the pack powder of 100% filling ratio. The NiAl coating almost completely consists of single NiAl phase with a small amount of AlN phase, because the reaction product of Al and air is only partly eliminated from the system. Based on the reaction during pack cementation with the traditional NH_4Cl activator[17], the possible reactions during pack cementation with $CaCl_2$ activator from initial temperature to over 780 °C are as follows:

$$2Al+3CaCl_2(l) \rightarrow 2AlCl_3(g)+3[Ca] \quad (2)$$

$$2AlCl_3(g)+Al \rightarrow 3AlCl_2(g) \quad (3)$$

$$AlCl_3(g)+2Al \rightarrow 3AlCl(g) \quad (4)$$

$$3AlCl_2(g) \rightarrow [Al]+2AlCl_3(g) \quad (5)$$

$$3AlCl(g) \rightarrow 2[Al]+AlCl_3(g) \quad (6)$$

$$Ni+[Al] \rightarrow NiAl \quad (7)$$

Al powder reacts with $CaCl_2$ to form gaseous $AlCl_3$ compounds and then gaseous AlCl and $AlCl_2$ are generated. AlCl and $AlCl_2$ are diffused to the specimen surface and the active Al atoms are released, thereby forming $AlCl_3$[18]. $AlCl_3$ repeatedly undergoes these reactions, resulting in continuous activation of the Al atoms. The released active Al atoms cause a concentration gradient of Al on the substrate surface and are diffused into the Ni substrate[19]. According to the NiAl binary phase diagram[20] (Fig. 2), the proportion of Ni and Al atoms participating in diffusion in this research is 1:1 near the diffusion interface, which is conducive to the formation of the NiAl phase. Because $CaCl_2$ has a high melting point and is in the molten state at the reaction temperature, the entire reaction process can be steadily promoted[21], resulting in the coating with uniform thickness and few defects.

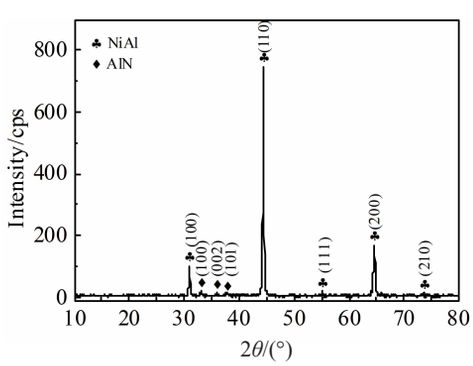

Fig.1 XRD pattern of NiAl coating

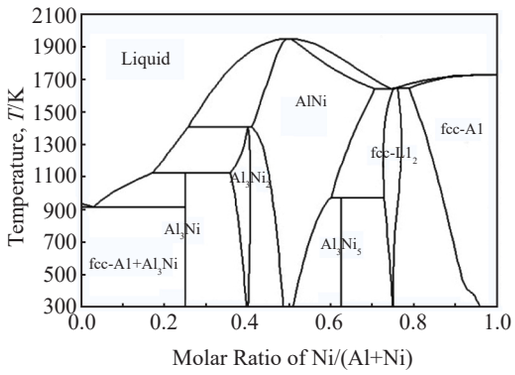

Fig.2 NiAl binary phase diagram[20]

Fig.3a shows the cross-section morphology of NiAl coating with the thickness of about 30 μm. The aluminized layer, diffusion layer, and the substrate can be observed from the surface to the interior specimen. EDS results show that the aluminized layer mainly consists of Ni and Al, which is in agreement with the XRD results. The diffusion layer contains numerous white particles with high Cr content. During the diffusion of Ni and Al atoms in the NiAl phase, the solid solubility of Cr and W in the substrate decreases. Cr and W are carbide-forming elements, so they can combine with carbon in the substrate and be precipitated in the diffusion layer in the form of carbides and chromium-rich precipitates[22]. The bonding interfaces have no obvious holes or defects. Fig. 3c shows SEM morphology of the NiAl coating surface, which consists of irregular particles of different sizes (0.5~2 μm), and the particle surface is smooth without oxide growth.

2.2 Effect of filling ratio of pack powder on NiAl coating structure

The SEM images in Fig. 4 show the surface morphologies of NiAl coating with pack powder of different filling ratios. The needle-like or grid-like θ-Al_2O_3 occurs on the coating surface. At filling ratio of 90%, only a little needle-like θ-Al_2O_3 can be observed on the coating surface (Fig. 4a). When the filling ratio decreases to 70%, many needle-like θ-Al_2O_3 particles grow on the coating surface; whereas the entire coating surface is covered by the needle-like θ-Al_2O_3 when the filling ratio is 50%. This is because when the filling ratio of the pack powder is less than 100%, some oxygen remains in the sealed crucible. When the active Al and Ni atoms diffuse to form the NiAl phase at high temperature, the oxidation process of Al atoms occurs at the diffusion interface. Owing to the simultaneous diffusion and oxidation processes, the in-situ formed θ-Al_2O_3 has a better combination with the coating[23], which improves the mechanical properties of NiAl coating, thereby effectively solving the problem of easy shedding of aluminum oxide layer.

2.3 Oxidation resistance behavior of NiAl-coated NiCrW-based superalloys

Fig. 5 shows XRD patterns of the NiCrW substrates after oxidation for different durations. After oxidation for 2~50 h, the diffraction peaks of Cr_2O_3 gradually appear and the

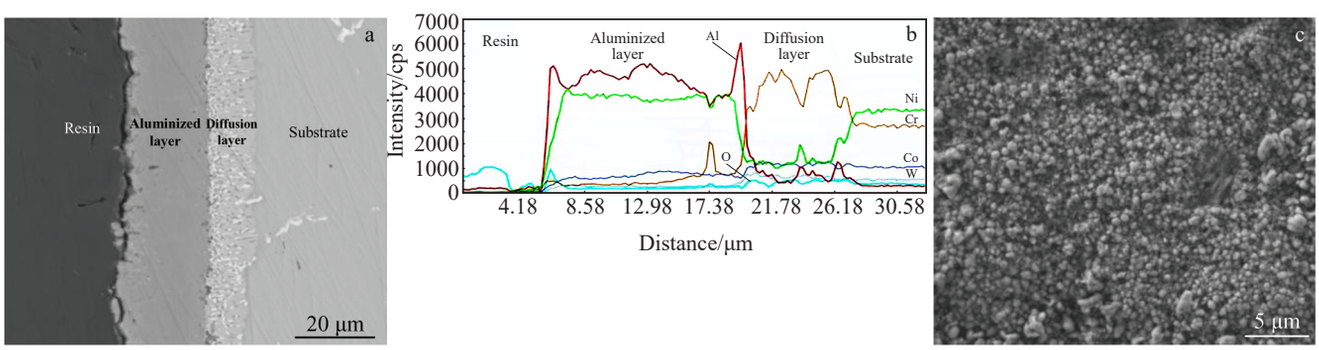

Fig.3 SEM morphology (a) and corresponding EDS line scanning results (b) of cross-section of NiAl coating; SEM surface morphology of NiAl coating (c)

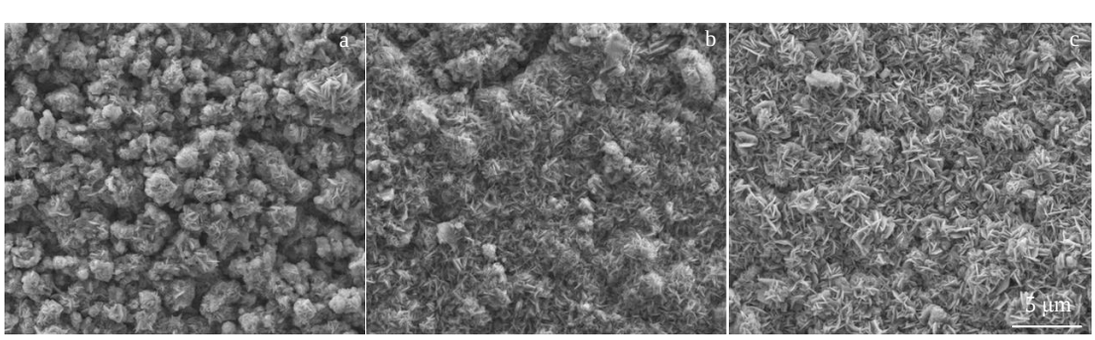

Fig.4 SEM surface morphologies of NiAl coating with pack powder of different filling ratios: (a) 90%, (b) 70%, and (c) 50%

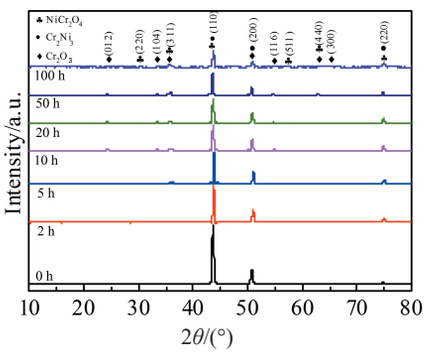

Fig.5 XRD patterns of NiAl-coated NiWCr-based superalloys after oxidation for different durations

intensity of each peak is increased. However, after oxidation from 0 h to 100 h, the intensity of the (110) and (200) main peaks of the Cr_2Ni_3 phase in NiCrW-based superalloys is decreased continuously. The diffraction peaks at 2θ=43.8° and 74.8° are composite peaks corresponding to Cr_2Ni_3 and $NiCr_2O_4$. After oxidation for 50 h, the (220) and (511) diffraction peaks of $NiCr_2O_4$ appear and the intensities of the (104) and (116) peaks corresponding to Cr_2O_3 are decreased. In addition, Cr_2O_3 can further react with O_2 to form volatile CrO_3. However, the amount of $NiCr_2O_4$ (product of NiO and Cr_2O_3) is increased during the oxidation process. Thus, the Cr_2O_3 content decreases, and the $NiCr_2O_4$ content increases.

EDS analyses of NiAl-coated NiCrW-based superalloys after oxidation for 100 h are shown in Fig.6. The products on the substrate surface are mainly irregular or sharp corner particles. The irregular particles mainly consist of O and Cr elements, and therefore are regarded as Cr_2O_3. The sharp corner particles mainly consist of O, Ni, and Cr elements, and therefore are regarded as $NiCr_2O_4$, which is formed by NiO and Cr_2O_3 during the late-stage oxidation of the Ni-rich substrate. $NiCr_2O_4$ can destroy the continuity of the previously formed Cr_2O_3 film. Moreover, the volume ratio of the oxide to the metal consumed for oxide formation, namely the Pilling-Bedworth ratio, of Cr_2O_3 and $NiCr_2O_4$ with spinel structure is large. A large internal stress is generated during the growth process[24]. In the early stage of oxidation, when the Cr_2O_3 film is thin, the internal stress can be released by deformation. However, after continuous oxidation, the oxide film becomes thick and $NiCr_2O_4$ is gradually formed. The deformation of this phase is increasingly difficult, and the internal stress of the film accumulates gradually[25]. When the internal stress exceeds the bonding strength of the Cr_2O_3 film, the oxide film breaks and peels off. Therefore, the formation of nickel-chromium spinel in the late-stage of oxidation reduces the protective effect of the oxide film on the substrate.

2.4 Oxidation resistance of NiAl coating

Fig. 7a shows the appearance of the specimen before oxidation. The specimen surface is relatively flat, and tightly combined with the matrix without obvious defects. Fig. 7b shows the appearance of the specimen after oxidation for 200 h. A large number of white oxides grow on the specimen surface. The NiAl coating covers the substrate evenly and densely, and it does not peel off.

Fig. 8 shows the XRD patterns of NiAl-coated NiCrW-based superalloys with filling ratio of 100% after oxidation for 200 h. After the constant temperature oxidation in air at 1000 °C for 5 h, a weak (110) diffraction peak of Al_2O_3 appears, indicating that oxidation starts and the nucleation of Al_2O_3 begins. After oxidation for 50 h, Al_2O_3 is formed considerably and a strong (110) peak can be observed. The Al_2O_3 phase grows up completely and appears as the main phase after oxidation for 200 h. Moreover, a small amount of intermediate product of $Al_{0.9}Ni_{4.22}$ phase is formed due to the Al oxidation.

Fig. 9 shows the surface morphologies of NiAl-coated NiCrW-based superalloys with filling ratio of 100% after oxidation for 100 and 200 h. The flaky θ -Al_2O_3 grows vertically on the coating surface due to the nucleation growth

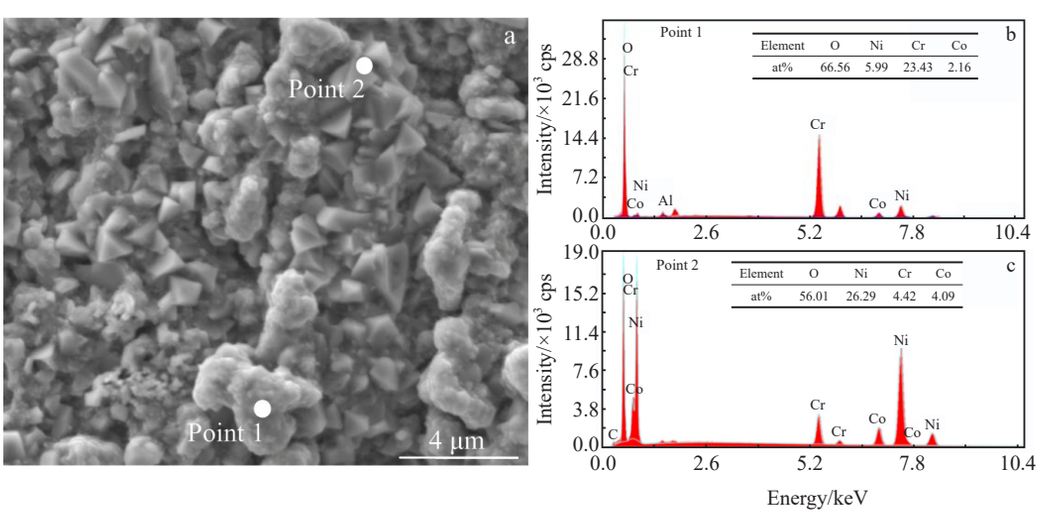

Fig.6 SEM morphology (a) and EDS analysis results of point 1 (b) and point 2 (b) in Fig. 6a of NiAl-coated NiCrW-based superalloys after oxidation for 100 h

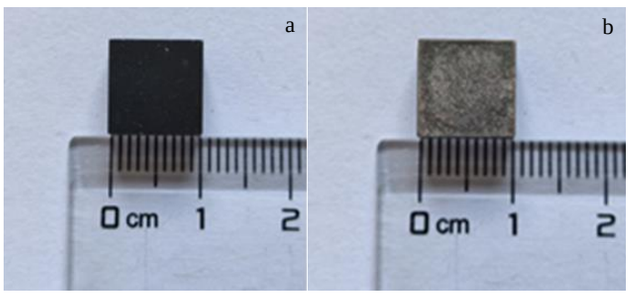

Fig.7 Appearances of specimen before (a) and after (b) oxidation for 200 h

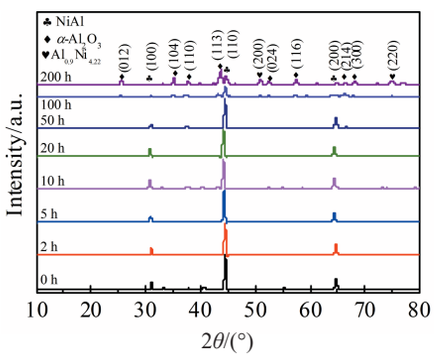

Fig.8 XRD patterns of NiAl-coated NiCrW-based superalloys with filling ratio of 100% after oxidation for different durations

of θ-Al_2O_3 at the early stage of oxidation. However, after oxidation for 200 h, many θ-Al_2O_3 flakes are transformed into irregular granular α-Al_2O_3. Compared with the vertically-disordered θ-Al_2O_3, the closely arranged α-Al_2O_3 better isolates the substrate from oxygen, leading to better high temperature oxidation resistance in the late stage and better anti-oxidation performance.

Fig. 10 shows the cross-sectional morphology of the NiAl coating after oxidation for 200 h. Compared with the initial NiAl layer (Fig.3a), an oxide layer with a thickness of about 4 μm is formed outside the NiAl coating. The EDS analysis results of different areas are shown in Table 2. The atomic ratio of Al to O in the oxide layer is 2∶3. Compared with the relatively flat coating surface in Fig.3a, the transition interface between the oxide layer and the coating is irregular, because of the non-synchronized oxidation of the coating caused by the chromium-rich precipitation, which hinders the Al diffusion in the NiAl layer. The aluminized layer is still dominated by the NiAl phase[26]. However, a residual chromium-rich phase and a tungsten-rich phase exist in the NiAl layer due to the diffusion and oxidation of Al. With the oxidation proceeding, the chromium-rich phase and tungsten-rich phase hinder the further diffusion of Al, thereby inhibiting the further oxidation[27].

Fig.11 shows the mass gain curves of NiAl-coated and non-coated NiCrW-based superalloys during oxidation. In the first 10 h of oxidation, the nucleation of Al_2O_3 occurs in the coated

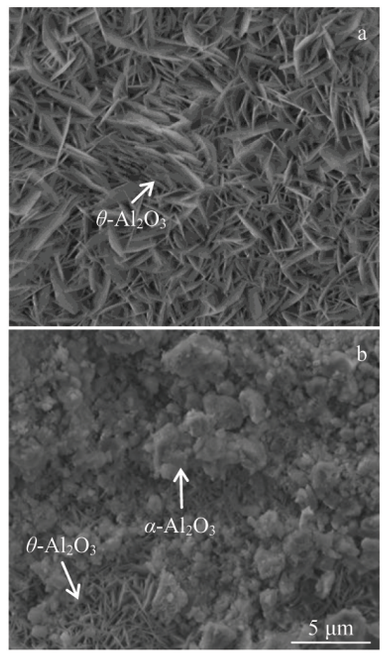

Fig.9 SEM surface morphologies of NiAl-coated NiCrW-based superalloys with filling ratio of 100% after oxidation for 100 h (a) and 200 h (b)

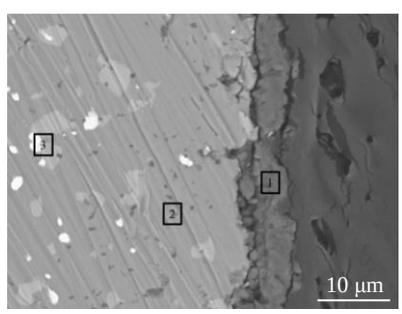

Fig.10 Cross-section morphology of NiAl coating after oxidation at 1000 °C for 200 h

Table 2 EDS analysis results of area 1, area 2, and area 3 in Fig.10 (at%)

Element	Area 1 (oxide layer)	Area 2 (aluminized layer)	Area 3 (precipitate phase)
O	56.1	1.3	7.6
Al	42.6	47.1	0.0
Cr	0.7	5.7	29.5
Co	0.0	5.5	17.9
Ni	0.6	40.2	17.5
W	0.0	0.0	27.4

specimens and the mass gain is relatively fast. With the oxidation further proceeding to 100 h, the specimens maintain a slow mass gain indicating that the oxidation enters into the stable growth period of θ-Al_2O_3. The transformation from

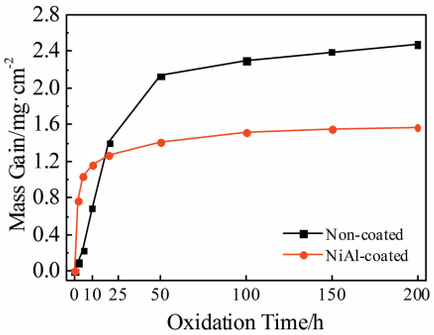

Fig.11 Mass gain curves of NiAl-coated and non-coated NiCrW-based superalloys during oxidation

θ-Al_2O_3 to α-Al_2O_3 occurs gradually during the oxidation process, leading to a gradual reduction in the oxidation mass gain of the specimen. Moreover, the mass gain increases slightly by 0.1 μg·cm^{-2}·h^{-1} during the oxidation from 150 h to 200 h, indicating that the NiAl coating exhibits good oxidation resistance after oxidation at 1000 °C for 100 h.

Furthermore, the fast oxidation rate of the NiAl coating during the early stage of oxidation results from the presence of the metastable θ-Al_2O_3. When the oxidation temperature is lower than 1050 °C, a certain oxygen partial pressure or water vapor environment is conducive to the formation and growth of θ-Al_2O_3[28]. The surface defects provide channels for the rapid ion migration which leads to the rapid oxide growth along the crystal surface[29], and appear in the metastable θ-Al_2O_3, resulting in the rapid growth of θ-Al_2O_3. Therefore, the growth rate of θ-Al_2O_3 in the first and middle stages of oxidation controls the oxidation process. With the oxidation proceeding, θ-Al_2O_3 gradually changes into stable α-Al_2O_3, forming a relatively dense alumina film, which inhibits the diffusion of oxygen and metal ions in the oxide layer. The growth of α-Al_2O_3 controls the late stage of the oxidation process, thereby leading to excellent oxidation resistance of the coating.

However, the substrate is a nickel-based chromium-rich alloy. In the early stage of oxidation, the formation of Cr_2O_3 film results in rapid mass gain of the substrate, but the thin Cr_2O_3 film has a weak protection effect on the substrate. With the oxidation further proceeding, the selective oxidation of Cr results in the formation of a nickel-rich area on the substrate surface, and $NiCr_2O_4$ with spinel structure and NiO are formed[30]. Therefore, the continuity of the Cr_2O_3 film is destroyed and the oxidation resistance of the oxidation film is reduced, which leads to a higher oxidation rate of the substrate, compared with that of the NiAl coating, in the late-stage of oxidation.

3 Conclusions

1) The NiAl coating containing 20wt% Al powder on NiCrW-based superalloys can be prepared by pack cementation at 950 °C for 4 h with $CaCl_2$ as the activator, and the thickness of NiAl coating is about 30 μm with a uniform structure and without obvious defects. The interlayer between the coating and the substrate is a chromium-rich phase diffusion layer.

2) The coating solely consists of single NiAl phase at the filling ratio of pack powder of 100%; the needle-like θ-Al_2O_3 grows on the surface of the nickel-based alloys at the filling ratio of pack powder of <100%.

3) Within the first 100 h of oxidation at 1000 ° C, the formation and growth of θ-Al_2O_3 mainly occur in the NiAl coating. After oxidation for more than 100 h, the mass gain of oxidation is decreased and then increased slightly with proceeding the oxidation. The metastable θ-Al_2O_3 is gradually transformed into dense and irregular granular steady-state α-Al_2O_3, which provides protection to the substrate in the late stage of oxidation process and leads to good oxidation resistance performance.

References

1 Wang Jian, Zhang Pingxiang, Hu Yue *et al*. *Rare Metal Materials and Engineering*[J], 2015, 44(5): 1169

2 Priest M S, Zhang Y. *Materials and Corrosion*[J], 2015, 66(10): 1111

3 Wang Y, Liu D W, Feng S J *et al*. *Surface and Coatings Technology*[J], 2016, 307: 271

4 Sun J, Fu Q G, Guo L P *et al*. *Materials & Design*[J], 2016, 92: 602

5 Shen T H, Tsai C Y, Lin C S. *Surface and Coatings Technology* [J], 2016, 306: 455

6 Liu Z J, Zhao X S, Zhou C G. *Corrosion Science*[J], 2015, 92: 148

7 Ou T P, Cao G H. *Transactions of Nonferrous Metals Society of China*[J], 2012, 22(6): 1725

8 Meng X X, Pei Y W, Wei S *et al*. *Corrosion Science*[J], 2018, 133: 112

9 Jiang J, Li R D, Yuan T C *et al*. *Materials Science and Engineering of Powder Metallurgy*[J], 2019, 24(2): 154

10 Wang Yao, Zhao Xueni, Dang Xinan *et al*. *Materials Reports*[J], 2018, 32(21): 3805 (in Chinese)

11 Liang Zhengang, Shen Mingli, Lu Xudong *et al*. *Journal of Functional Materials*[J], 2015, 46(13): 106 (in Chinese)

12 Zielinska M, Sieniawski J, Yavorska M *et al*. *Archives of Metallurgy and Materials*[J], 2011, 56(1): 193

13 Sitek R. *Vacuum*[J], 2019, 167: 554

14 Philippe T, Erdeniz D, Dunand D C *et al*. *Philosophical Magazine*[J], 2015, 95(9): 935

15 Patrick J M, Agnieszka B, Jan S *et al*. *Defect and Diffusion Forum*[J], 2010, 23(3): 381

16 Lu T, Yao D Z, Zhou C G. *Chinese Journal of Aeronautics*[J], 2010, 23(3): 381

17 Fan Q X, Jiang S M, Wu D L *et al*. *Corrosion Science*[J], 2013, 76: 373

18 Wang Q Y, Xi Y C, Xu J *et al*. *Journal of Alloys and Compounds*

[J], 2017, 729: 78
19 Qiao M, Zhou C G. *Corrosion Science*[J], 2013, 75: 454
20 Meng Caisi, Huo Keli, Chen Zhong *et al*. *Equipment Environmental Engineering*[J], 2019, 16(1): 13 (in Chinese)
21 Cai Huai. *Thesis for Master*[D]. Harbin: Harbin Institute of Technology, 2017 (in Chinese)
22 Cheng Xiaonong, Jiang Yang, Li Dongsheng *et al. Journal of Functional Materials*[J], 2013, 44(12): 1792
23 Miu Weiliang. *Thesis for Master*[D]. Harbin: Harbin Institute of Technology, 2017 (in Chinese)
24 Zhou Y H, Zhao X F, Zhao C S *et al*. *Corrosion Science*[J], 2017, 123: 103
25 Khan A, Huang Y, Dong Z *et al*. *Corrosion Science*[J], 2019, 150: 91
26 Cao J D, Gong S J, Zhong C G *et al*. *Rare Metal Materials and Engineering*[J], 2018, 47(12): 3616
27 Sophia A T, Elena G. *Materials Characterization*[J], 2016, 118: 494
28 Liu L, Yu S R. *Corrosion Science*[J], 2017, 123: 103
29 Yao Yanbin, Hua Yinqun, Tong Fuli. *Hot Working Technology*[J], 2018, 7(10): 175 (in Chinese)
30 Pourasad J, Ehsani N. *Journal of Alloys and Compounds*[J], 2017, 690: 692

包埋法制备NiAl涂层NiCrW基高温合金的抗氧化性能

高　杉[1]，邹俭鹏[1,2]
(1. 中南大学 粉末冶金国家重点实验室，湖南 长沙 410083)
(2. 大功率交流传动电力机车系统集成国家重点实验室，湖南 株洲 412001)

摘　要：以$CaCl_2$为活化剂，采用包埋法在NiCrW基高温合金表面制备了NiAl涂层。采用X射线衍射、扫描电子显微镜和能谱仪对涂层表面和横截面进行了分析。结果表明，$CaCl_2$可以替代NH_4Cl，是一种有效的活化剂。在950 ℃下，通过4 h的包埋渗铝，制备出几乎为单相、厚度为30 μm的NiAl涂层，涂层与基体之间为富铬中间层。当包埋渗剂填充率小于100%时，NiAl层表面生成针状θ-Al_2O_3。在1000 ℃恒温空气氧化试验中，NiAl涂层开始时被高速氧化，然后逐渐变为缓慢氧化，完成了亚稳态针状θ-Al_2O_3向稳态不规则颗粒状α-Al_2O_3的转变，最终稳定的α-Al_2O_3为基体提供了良好的抗氧化保护。

关键词：NiCrW基高温合金；NiAl涂层；包埋法；抗氧化

作者简介：高　杉，男，1996年生，硕士生，中南大学粉末冶金国家重点实验室，湖南 长沙 410083，电话：0731-88876630，E-mail：zoujp@csu.edu.cn